Transcriptionally-correlated sub-cellular dynamics of MBNL1 during lens development and their implication for the molecular pathology of Myotonic Dystrophy Type 1.

Stewart M. Coleman*, Alan, R. Prescott†, Judith E. Sleeman*.
*University of St Andrews, School of Biology, BSRC Complex, North Haugh, St Andrews, UK, KY16 9ST. †University of Dundee, College of Life Sciences, Dundee, UK, DD1 5EH.

Corresponding author: Judith E Sleeman, University of St Andrews, School of Biology, BSRC Complex, North Haugh, St Andrews, UK, KY16 9ST. Tel: +44 (0)1334 463524, jes14@st-andrews.ac.uk.
[1]

[1] Abbreviations: ASF, alternative splicing factor; 5-BrU, 5-bromouridine; Cy5, cyanine 5; DM1, Myotonic Dystrophy Type 1; DMEM, Dulbecco's modification of Eagle's medium; DMPK, dystrophia myotonica protein kinase; DRB 5,6-Dichloro-1-β-D-ribofuranosylbenzimidazole; FISH, fluorescent in situ hybridization; HLE, human lens epithelial; LEC, lens epithelial cell; MBNL1, muscleblind-like protein 1; PAGFP, photoactivatable GFP; PFA, paraformaldehyde; SC35, splicing component 35kDa; snoRNP, small nucleolar ribonucleoprotein; snRNP, small nuclear ribonucleoprotein; SSA, spliceostatin A; SSC, saline sodium citrate.

Abstract

Myotonic Dystrophy Type 1 (DM1) is caused by elongation of a CTG repeat in the dystrophia myotonica protein kinase (DMPK) gene. mRNA transcripts containing the resulting CUG^{exp} repeats form accumulations, or foci, in the nucleus of the cell. The pathogenesis of Myotonic dystrophy type 1 (DM1) is proposed to result from inappropriate patterns of alternative splicing caused by sequestration of the developmentally regulated alternative splicing factor muscleblind-like 1 (MBNL1), by these foci. Since eye lens cataract is a common feature of DM1 we have examined the distribution and dynamics of MBNL1 in lens epithelial cell lines derived from DM1 patients. The results demonstrate that only a small proportion of nuclear MBNL1 accumulates in CUG^{exp} pre-mRNA foci. MBNL1 is, however, highly mobile and changes sub-cellular localization in response to altered transcription and splicing activity. Moreover, immunolocalization studies in lens sections suggest that a change in MBNL1 distribution is important during lens growth and differentiation. While these data suggest that loss of MBNL1 function due to accumulation in foci is an unlikely explanation for DM1 symptoms in the lens, they do demonstrate a strong relationship between sub-cellular MBNL1 localisation and pathways of cellular differentiation, providing an insight into the sensitivity of the lens to changes in MBNL1 distribution.

Short title: MBNL1 dynamics in lens epithelial cells from myotonic dystrophy patients

Summary Statement: In eye lens cells from DM1 patients MBNL1 sequestration to RNA foci appears not to be a major pathological event. MBNL1 does, however, show clear changes in sub-cellular distribution related to transcriptional activity and cellular differentiation.

Keywords: Differentiation; DM1; Lens epithelium; MBNL1; Nuclear dynamics; Splicing Speckles

Introduction

Myotonic dystrophy type 1 (DM1) is a genetic condition resulting in multiple symptoms including skeletal muscle wasting, cardiac conduction defects, myotonia, cataracts and endocrine system malfunction. The fundamental molecular defect underpinning the pathogenesis of DM1 is the elongation of a CTG repeat in the 3'UTR of the dystrophia myotonica protein kinase (DMPK) gene on chromosome 19.3.3q [1]. DMPK RNA containing the consequent CUG expansion has been demonstrated to form abnormal foci within the cell nucleus in muscle cells from DM1 patients [2, 3]. The link between these CUGexp RNA foci and the multiple symptoms of DM1 is not fully understood. Muscleblind-like (MBNL) proteins are a family of alternative splicing regulators that show tissue-specific expression and regulation. The alternative pre-mRNA splicing factor muscle blind-like 1 (MBNL1), which is known to regulate alternative splicing events in many pre-mRNAs such as Cardiac tropinin T (cTNNT) and Insulin receptor (IR) [4, 5], is found in the CUGexp foci [6] in DM1 muscle cells. This has lead to the hypothesis that sequestration of MBNL1 by the elongated CUG containing pre-mRNA and consequent mis-regulation of MBNL1-dependant splicing is a key factor in DM1 pathogenesis. MBNL1 also has a number of different functions in mRNA metabolism in addition to its role in alternative splicing. The accumulation of MBNL1 within cytoplasmic stress granules suggests a role in chaperoning mature, spliced mRNA[7], with a recent report revealing extensive binding of MBNL proteins to the 3' untranslated regions (UTRs) of mRNAs and demonstrating widespread roles for MBNL proteins in regulating mRNA localization in both Drosophila and mice[8]. A regulatory role for MBNL1 during cell differentiation and development has also been suggested. During early mouse development, MBNL1 is predominantly cytoplasmic in skeletal muscle at P2 and predominantly nuclear in the same tissue at P20 [9]. Changes in cellular distribution of MBNL1 between the nucleus and cytoplasm have been observed in cultured mouse myoblasts, although these changes were shown not to be correlated to differentiation[10]. The control of alternative splicing patterns by MBNL1 has now been implicated in the negative regulation of pluripotency in mouse embryonic stem cells, giving it a central role in the determination of cell fate during early stages of differentiation[11].

Pre-senile cataracts are almost always the first and sometimes the only sign of DM1 [12] although the specific pathogenic pathway that results in cataract development has yet to be determined. The related condition, Myotonic dystophy type 2 (DM2) is caused by a CCTG repeat in intron 1 of Zinc Finger Protein 9 (ZNF9) gene on chromosome 3q21[13]. The similarity in the cataracts symptomatic of DM1 and DM2 patients suggests a common pathogenic pathway. In muscle cells from both DM1 and DM2 patients, MBNL1 is sequestered into nuclear RNA foci formed by CUG and CCTG repeats sequences respectively[6, 14]. This strongly suggests that the sequestration of functional MBNL1 by the CUG^{exp}-containing pre-mRNA contributes to cataract development as well as other symptoms of DM1. The eye lens consists of two cell types: an anterior simple epithelium that covers the anterior portion of the lens below the capsule and elongated fibre cells which make up the bulk of the lens and are derived from the differentiation of epithelial cells forming a stem cell pool at the lens equator[15]. Because the lens retains all the cells it produces during development and into adulthood a thin transverse

section of the lens contains cells at all stages of differentiation. Changes in organization of the cell nucleus can be correlated with the transcriptional activity of cells at different stages of differentiation. Notably up-regulation of transcription is seen during post-mitotic differentiation steps in the equatorial epithelium and differentiation from epithelium to fibre cells at the lens equator while transcriptional shutdown is observed prior to nuclear elimination in the outer cortical fibre cells[16, 17]. Several nuclear proteins change their distribution in response to these changes in transcriptional activity. For instance upon transcriptional up-regulation the nucleolus, as followed with the snoRNP (small nucleolar ribonucleoprotein) protein fibrillarin, changes from a closed structure to an open floret-like structure. In the same cells the distribution of the Cajal body marker, coilin, changes from single large structures to multiple small structures with increased diffuse nucleoplasmic staining[18]. The availability of human lens epithelial (HLE) cell lines and intact mammalian lenses, in which progressive stages of differentiation of lens epithelial cells can be mapped, makes the lens an ideal biological system to investigate the molecular pathology associated with DM1 with particular relevance for the formation of the characteristic cataracts seen in DM1 patients.

In this study, we have used a unique set of human lens epithelial (HLE) cell lines, derived from DM1 patients and age-matched controls to investigate the localization and dynamics of MBNL1 in different regions of the cell. Together with parallel studies of lens sections, our data demonstrate that the sub-cellular distribution of MBNL1 is highly dynamic, changing during HLE cell differentiation and according to the transcriptional activity of the cell. Regardless of the overall cellular distribution of MBNL1, the proportion of the protein recruited by the CUG^{exp} RNA foci is extremely small making it unlikely that a loss of functional MBNL1 due to its sequestration within the foci is a major cause of the cellular pathology of DM1 within the lens. We propose that the characteristic cataracts seen in DM1, and perhaps other symptoms, may result from defects in programmes of cellular differentiation, caused by subtle disturbances in the balance between the functions of MBNL1 in pre-mRNA splicing and mRNA chaperoning and localization. Furthermore, we demonstrate a reduction in the accumulation of MBNL1 into CUG^{exp} RNA foci following the inhibition of pre-mRNA splicing. This is associated with an apparent reduction in size of the foci themselves, suggesting a potential avenue for investigation into therapies for DM1 involving dismantling the foci.

Experimental

Cell lines and Cell Culture

DM1 and age matched control human lens epithelial cell lines were derived by SV40 transformations of human lens epithelial specimens, obtained from DM1 patients following capsulorhexis and non-cataractous donor lenses post mortem as published previously[19]. Lines DMCat1 to DMCat4 are derived from DM1 patients, CCat1 and CCat2 are control lines. All cells were maintained in Dulbecco's Modified Eagle Medium (DMEM) supplemented with 10% Foetal Bovine serum (FBS) and 100 units Penicillin + 0.1mg/ml Streptomycin (Life Technologies) at 37°C in 5% CO_2. When appropriate**,** 20μg/ml 5,6-dichloro-1-β-d-ribofuranosylbenzimidazole (DRB) (Sigma) or 25ng/ml Spliceostatin A (SSA) (a gift from M. Yoshida, RIKEN, Japan) was added the growth medium of the cells for the times indicated. Transfection with DNA plasmids was carried out using X-treme GENE HP DNA (Roche) reagent according to manufactures instructions. To assay for transcriptional activity, HLE cells were cultured till 60% confluent on 18mm square coverslips. The cells were incubated for 2 hours with 1mM 5-ethynyl uridine (EU, Life Technologies), fixed using 3.7%PFA, the incorporation of EU into RNA assayed using a Click-iT RNA alexa-fluor 594 imaging kit (Life Technologies) and the cells simultaneously immunostained using anti-MBNL1.

Plasmid Constructs

pmCherry-ASF and pmCherrySC-35 [20] were a gift from A. Lamond, (University of Dundee, UK). pEGFP-MBNL1-N1 [14] was a gift from T.Cooper (Baylor College of Medicine Houston, TX). pPAGFP-MBNL1 was generated by replacing EGFP in vector pEGFP-MBNL1-N1 with PAGFP [21] (a gift from J. Lippincott-Schwartz, NIH, Bethesda, MA) using AgeI and BsrGI restriction enzymes (New England Biolabs).

Cell Fixation, Immunostaining and Image Analysis

Cells were cultured on 18mm square coverslips and fixed for 10 minutes at room temperature with 3.7% paraformaldehyde in PHEM buffer [60 mM Pipes, 25 mM Hepes, 10 mM EGTA, 2 mM $MgCl_2$ (pH 6.9)]. Immunostaining was carried out as described previously[22]. Coverslips were mounted using ProLong® Gold antifade reagent (Life Technologies). Antibodies used were MBla (mouse monoclonal anti-MBNL1), dilution 1:25, a gift from G. Morris, RJAH Orthopaedic Hospital, Oswestry, UK[10]; 856 (rabbit polyclonal ant-U1A), dilution 1:500, a gift from I. Mattaj, EMBL, Heidelberg[23]; FITC and TRITC goat anti-mouse and TRITC and Cy5 goat anti-rabbit, dilution 1:500 (Jackson Research Laboratories) . Cells were imaged using a 100x, 0.35na objective on an Olympus DeltaVision RT microscope (Applied Precision) with 2x2 binning and 0.2μm intervals for Z-stack series. Exposure times using DAPI, FITC, TRITC and Cy5 filter sets were chosen to aim for maximum intensities of 3600 in each z-series. Deconvolution was carried out using Volocity 4 image analysis software (Perkin Elmer) with calculated point-spread functions. To quantify proportion of nucleoplasmic MBNL1 within foci, MBNL1 intensity threshold was used to create 3D regions of interest encompassing only foci (Volocity), this was confirmed by visual inspection. Total nucleoplasmic MBNL1 was quantified as the sum of MBNL1 intensity within the boundaries of the nucleus as defined by DAPI staining. Background intensity was subtracted from both regions and the sum MBNL1 intensity in foci was expressed as a percentage of sum total of nucleoplasmic MBNL1. To quantify the ratio of MBNL1 with in the cytoplasm, Phalloidin 568 (Molecular Probes) staining was used to identify the total cell volume. To quantify

transcriptional activity, the volume of the nucleus was defined using DAPI signal. To assess MBNL1 accumulation in speckles, Pearsons colocalisation coefficient was used to measure the linear correlation between pixel colocalisation from the two wavelengths, as described by the equation below. If the correlation coefficient has the value r=1 the two images are absolutely identical.

$$r = \frac{\sum_i (x_i - x_m)(y_i - y_m)}{\sqrt{\sum_i (x_i - x_m)^2}\sqrt{\sum_i (y_i - y_m)^2}}$$

Pearsons correlation coefficient equation; Where x_i is the intensity of the ith pixel in image 1, y_i is the intensity of the ith pixel in image 2, xm is the mean intensity of image 1, and y_m is the mean intensity of image 2

Lens Transverse Section Analyses

Pig eyes were collected fresh from the abattoir and the lenses were removed by entering the eye from the posterior aspect. The lenses were frozen in iso-pentane cooled to liquid nitrogen temperature and stored at -80°C until required. Frozen 20μm thick transverse cryo-sections (Leica CM3050S) were taken across the centre of the lens to include cells at all stages of differentiation. The sections were fixed in 3.7% PFA in PBS and permeabilized with 0.5% Triton X100 in PBS. Following blocking with 1% normal goat serum the sections were incubated with primary antibodies, washed then incubated with secondary antibodies to which DAPI had been added. Stained sections were mounted in ProLong Gold (Life Technologies) and imaged on a DeltaVision Spectris deconvolution microscope (Applied Precision). Images were analysed using Volocity 4 (Perkin Elmer).

Fluorescence *in-situ* hybridisation FISH

Cells fixed with 3.7% PFA in PHEM buffer were permeabilized with 1% v/v Triton X-100/PBS for 10mins at room temperature. PBS was treated with 0.1% v/v Diethylpyrocarbonate (DEPC). Cells were blocked using 1% Goat serum/ PBS for 15mins before addition of primary antibodies diluted in 1% Goat serum/PBS. Coverslips containing the cells were placed into a humidified chamber and incubated for 1 hour at 37°C. Following three x 10 minute washes with PBS, cells were incubated with secondary antibodies was diluted in 1% Goat serum/ PBS for 1hour at 37°C. Cells were refixed with 3.7% PFA for 1min and incubated in 50% Formamide /2X SSC for 10mins at room temperature before addition of 200ng/ml Cy3-labelled GAC_{10} DNA probe (5'-/5Cy3/$(CAG)_{10}$) (IDT) diluted in pre warmed hybridization buffer (40% (v/v) Formamide + 20% (w/v) BSA + 50% (w/v) Dextran sulphate +2mM Vanadyl adenosine complexes + 1mg/ml tRNA bakers yeast + 1mg/ml salmon sperm DNA (all Sigma)). Following incubation for 3hours at 37°C, the cells were washed in 2X SSC for 2*10mins then 0.2X SSC for 10mins before a final wash in PBS for 5mins. Cells were counterstained with DAPI and the mounted using ProLong® Gold antifade reagent (Life Technologies).

Live Cell Imaging

For live cell experiments, cells were cultured on 40mm glass coverslips (Intracel). The coverslips were transferred to an open chamber (Zeiss) within an environmental

incubator (Solent Scientific, Segensworth, UK) on an Olympus DeltaVision RT microscope (Applied Precision) with a quantifiable laser module including a 488 nm and 405 nm lasers, and maintained at 37°C with 5% CO_2. Transfected cell expressing GFP tagged proteins were identified using FITC filters, mCherry tagged proteins were identified using TRITC filters. Z-stacks of images separated by 500nm were collected at approximately 3-minute intervals using a 100X 1.35na objective. Exposure times were optimized to give a maximum intensity value of ~500 in each z-series. For measurements of distance between foci and speckles, foci (GFP-MBNL1) and speckles (mCherrySC-35) were identified by % intensity and object size using Volocity 4 (Perkin Elmer).

FRAP and PA-GFP analyses

A 488nm laser was used to Photobleach GFP-MBNL1 with a 0.5sec pulse at 100% power, in specific areas of the cells. The photobleaching was optimised to achieve ~60% reduction in fluorescence. A single Z-section of each cell was imaged 3 times prior to bleaching, using a 100X 1.35na objective and FITC filters. Post bleaching imaging used adaptive intervals for 48 time-points. Images were normalized against pre-bleach florescence intensity. FRAP recovery curves were generated from background-subtracted images. One-phase exponential association curves were fitted the mean of data sets for each cell line (GraphPad Prism). Equation used: Y=Ymax x (1-exp(-K x X)).

Cells transfected with PAGFP-MBNL1 were identified using a DeltaVision RT microscope with a PAGFP eyepiece filter (405/40nm). PAGFP-MBNL in the region of interest was activated using a 405nm laser with a 0.5sec pulse at 100% power. Three pre-activation images and 55 adaptive time interval images were acquired using a 100X 1.35na objective and FITC filters.

Statistical analysis

All statistical analyses were performed using Prism 4 software (GraphPad).

Results

1) Lens epithlial cells from DM1 patients contain CUG RNA foci that accumulate MBNL1

The presence of CUG^{exp} RNA foci within the nuclei of cells is recognized as a key hallmark of cells in DM1 patients, with colocalization of MBNL1 and CUG^{exp} mRNA thought to be fundamental to the molecular pathogenesis of DM1. To asses the potential of lens epithelial cell lines derived from DM1 patients as a model to study the localization and dynamics of the alternative splicing factor, MBNL1, we sought to identify the CUG RNA foci and to asses the co-localization of both endogenous and GFP-tagged MBNL1 (a gift from Prof. T. Cooper, [4] with them (figure 1). After first confirming that DMPK1 mRNA is present in lens epithelial cells using reverse transcriptase PCR, we carried out florescence in situ hybridization (FISH) using a Cy3 labeled GAC_{10} DNA probe combined with Immunocytochemistry using an antibody to endogenous MBNL1 (a gift from Prof. G. Morris). This demonstrated that CUG^{exp} mRNA forms clear foci that recruit endogenous MBNL1 within the nuclei of DM1 HLE cells (figure 1A, arrows). Control HLE cells (figure 1C) do not demonstrate RNA foci, or punctate accumulations of endogenous MBNL1. Parallel experiments carried out in cells transiently transfected with a plasmid to express GFP-MBNL1 confirmed the accumulation of GFP-tagged MBNL1 in the CUG^{exp} RNA foci in DM1 cells (figure 1B). No spontaneous aggregation of GFP-MBNL1 was observed in control cells (figure 1D). Importantly, statistical analysis of the number of foci per nucleus revealed no significant differences between the number of foci seen per nucleus in cells expressing GFP-MBNL1 and in untransfected cells (figure 1E). This indicates both that exogenous expression of MBNL1 does not increase the formation of CUG^{exp} RNA foci and that GFP-MBNL1 can be used as a marker for the foci in living cells.

2) MBNL1 has a complex sub-cellular localization in lens epithelial cells

Although MBNL1 is recognized as an alternative splicing factor[9, 24], additional, extra-nuclear roles for MBNL1 in the regulation of mRNA localization and protein expression have recently been implicated in the pathology of DM1[8]. In normal HLE cells, endogenous MBNL1 shows a complex subcellular distribution (figure 2A) with staining both in the nucleus and the cytoplasm. The nuclear signal is largely excluded from the nucleolus (figure 2A arrows). The only clear difference in the distribution of MBNL1 in DM1 cells compared to control cells is the presence of the distinctive foci (Figure 2A yellow arrows). Of particular interest is the non-uniform distribution of MBNL1 within the nucleus in some, but not all, cells where MBNL1 accumulates in structures resembling splicing factor 'speckles' (figure 2A arrowheads). While this is not unexpected, as MBNL1 has a well-documented role as an alternative splicing factor and splicing factors characteristically accumulate in speckles[25], it has not been documented previously. We therefore sought to confirm the identity of the structures accumulating MBNL1. Immunodetection of the U1 snRNP associated protein, U1A simultaneously with endogenous MBNL1 in normal HLE cells demonstrates conclusively that the structures seen to accumulate MBNL1 are canonical splicing speckles (figure 2B). Equivalent results were obtained in DM1 HLE cells (data not shown). In addition to the observation of cells with diffuse nuclear staining with MBNL1 (DM1 75.5%, sem +/- 0.5; control 77.5%, sem +/- 1.5) and cells with MBNL1

accumulated in nuclear splicing speckles (DM1 21%, sem +/-2.0; control 19% sem +/-2.0), a small number of cells with very little nuclear MBNL1 and cytoplasmic accumulations of MBNL1 were also observed (DM1 4%, sem+/- 0.0; control 4%, sem +/-1.0).

3) MBNL1 moves between the nucleus and cytoplasm during lens development

Porcine lens sections stained with MBNL1 and the snRNP splicing factor U1A (Figure 3A) show that, while the constitutive splicing factor U1A remains nuclear throughout lens cell differentiation, MBNL1 shows changes in sub-cellular distribution during fibre cell differentiation. MBNL1 is present in both the nucleus and the cytoplasm in cells in the anterior epithelium known to have low transcriptional activity (figure 3A, top row), but is increasingly nuclear in cells of the equatorial epithelium and cortical fibre cells, where high transcriptional activity has previously been reported (figure 3A middle and bottom rows). Further examination of the cortical fibre cells (figure 3B) demonstrates partial co-localization of MBNL1 (ii) with U1A (i) in nuclear speckles (arrows). Staining of the actin cytoskeleton with phalloidin 568 (iv) clearly shows the elongated structure of the differentiating fibre cells.

4) MBNL1 localizes to the cytoplasm in cells with low transcriptional activity

To further investigate the potential link between transcriptional activity and MBNL1 distribution suggested by the results from lens sections, we next sought to determine if the distribution of MBNL1 in HLE cell lines was related to the level of cellular transcription. DM1 and control HLE cells were incubated with 5-ethynyl uridine (EU) for two hours to allow incorporation of the label into newly synthesized RNA. Subsequent detection of the EU label using 'click' chemistry and endogenous MBNL1, suggested that cells with nuclear MBNL1, whether diffuse or in splicing speckles (arrows), are highly transcriptionally active (figure 4A). Newly synthesized transcripts were detected both in the nucleoplasm (RNA polymerase II transcription) and in nucleoli (figure 4A, B) yellow arrows, RNA polymerase I transcription). In contrast, cells without strong nuclear localization of MBNL1 and with cytoplasmic accumulations of MBNL1 (figure 4B, arrowheads) showed low transcriptional activity in both the nucleoplasm and nucleoli. While high variability of signal intensity between coverslips prevents a definite quantitative conclusion from being drawn, viewing cells with different distributions of MBNL1 in the same image (figure 4B) gives a clear indication of the relative transcriptional activities. These observations are in agreement with our results in lens sections and suggest that the distribution of MBNL1 between the cytoplasm and nucleus is linked to the transcriptional activity of the cell reflecting the balance between different proposed roles for MBNL1 in mRNA metabolism.

5) The proportion of cellular MBNL1 in nuclear CUGexp RNA foci is small.

The sequestration of MBNL1 in CUG^{exp} RNA foci has been implicated as a key cause of the cellular pathology seen in DM1. To assess the extent of MBNL1 sequestration in DM1 HLE cells, immunostaining with anti-MBNL1 was used. To define the different regions of the cells, they were counter-stained with DAPI to identify the nucleus, and

phalloidin 568 to identify the filamentous actin cytoskeleton, defining the boundary of the cell. Optical sections at 0.2μm spacing were collected throughout the cell and these datasets used to quantify the proportion of endogenous MBNL1 in each region of the cell using Volocity (Perkin Elmer). These analyses demonstrate that only ~0.2% of total endogenous MBNL1 is sequestered in the foci, whereas ~40% of MBNL1 is localized in the nucleus (figure 5A) and ~60% in the cytoplasm. As the pathogenesis of DM1 is thought to result from a reduction in the availability of nuclear MBNL1 and consequent disruption of alternative splicing patterns, the proportion of nuclear MBNL1 sequestered in foci was calculated. Only ~0.5% of nuclear MBNL1 is sequestered into the foci, demonstrating a very small reduction in the potential availiblilty of MBNL1 within the nucleus in DM1 HLE cells (figure 5B). Parallel experiments using GFP-MBNL1 in place of endogenous MBNL1 gave similar results with ~0.1% of nuclear GFP-MBNL1 sequestered into foci. This suggests that the sequestration of MBNL1 in the foci is limited by the number of available binding sites, with additional expressed GFP-MBNL1 localizing within the nucleoplasm rather than causing an increase in the size or number of the foci.

6) MBNL1 in foci, and the foci themselves, are mobile.

Having established that the proportion of MBNL1 present in CUG^{exp} pre-mRNA foci is small, we next sought to investigate whether the foci-bound MBNL1 was able to disassociate from the foci. Fluorescence recovery after photobleaching (FRAP) was used in DM1 HLE cells expressing GFP-MBNL1 to determine the mobility of sequestered MBNL1 (figure 6A). Photo-bleaching of GFP-MBNL1 in foci with a 488nm laser and analysis of the migration of unbleached GFP-MBNL1 into the bleached area gave a mobile fraction of ~50%, suggesting about half of the GFP-MBNL1 found in foci is free to dissociate and is not permanently bound by the CUG^{exp} mRNA foci. These data are in broad agreement with previous studies of the interaction of GFP-MBNL1 with artificial CUG^{exp} foci in muscle cells[14]. To further investigate the dynamics of MBNL1 in foci, DM1 HLE cells were transiently transfected with photoactivatable GFP-MBNL1 (PAGFP-MBNL1). Nuclei containing more than one focus were selected and one focus per nucleus activated using a 405nm laser. Subsequent time-lapse imaging of the nuclei showed the migration of PAGFP-MBNL1 (figure 6B) within the nucleus and its accumulation in foci distant from the activated focus. This demonstrates that MBNL1 can exchange between different foci as well as between the foci and the nucleoplasm. It has been suggested that the CUG^{exp} RNA foci represent a block in an early stage of mRNA export from the nucleus with foci being physically stuck at the periphery of speckles[10, 26]. DM1 HLE cells expressing GFP-MBNL1 and the speckle marker protein, SC35, tagged with mCherry (mCherrySC35) were used for time-lapse imaging to investigate the relationship between foci and speckles. The resulting time series reveal a more complex picture than anticipated from previously published data. While some foci did remain in close proximity to a single speckle over the 15-minute period imaged (figure 6C, arrows), other foci appeared to be free to travel within the nucleus (figure 6C, arrowheads, see also supplementary movie 1). Plotting of the minimum distances between a given CUG^{exp} focus and its nearest mCherrySC35 speckle against time clearly demonstrates the variety of movements seen (figure 6C). Taken together, these data show that the foci are, in fact, highly dynamic. MBNL1 protein is in constant

equilibrium within foci, while some of the foci themselves have the ability to move within the nucleus with no clear connection to nuclear speckles.

7) Experimental Inhibition of transcription does not affect the accumulation of MBNL1 in RNA foci, but causes migration of MBNL1 out of the nucleus.

The MBNL1 protein is clearly highly dynamic within the cell, showing a complex transcription-related distribution both *in vitro* and *in vivo* and rapid exchange between cellular compartments. Understanding the molecular basis for the maintenance of CUG^{exp} foci in DM1 cells is likely to be of key importance to understanding the condition. To further investigate the relationship between cellular transcriptional activity and the RNA/MBNL1 foci, 5,6-Dichloro-1-β-D-ribofuranosylbenzimidazole (DRB), was used to inhibit transcription in DM1 HLE cells. Detection of the RNA foci by fluorescence in situ hybridization (FISH) in cells fixed at different time intervals after DRB addition demonstrates that the number of foci per nucleus is unaffected by global inhibition of transcription over a five hour time-course (fig 7 A and B). In order to directly observe the effect that inhibition of transcription by DRB has on MBNL1 distribution over time, HLE cells from DM1 patients were transiently transfected with plasmids to express GFP-MBNL1 and mCherry-ASF, an alternative splicing factor and common marker for speckles. The transfected cells were treated with DRB (Fig 7 C). Time-lapse imaging of these cells shows that, while mCherry-ASF shows the expected gradual change in localization from angular splicing speckles to rounded-up structures characteristically seen in transcriptionally inhibited cells[27, 28], GFP-MBNL1 shows a relocalization from the nucleus to the cytoplasm. Importantly, GFP-MBNL1 remains in nuclear foci (arrows) throughout the time course. The transcriptional inhibition caused by DRB is reversible, and the alterations to the distribution of mCherry-ASF and GFP-MBNL1 show reversion over a similar time-frame (fig 7C). These observations demonstrate conclusively that the sub-cellular distribution of MBNL1 is dependent on the transcriptional activity of the cell but that ongoing transcription is not required for maintenance of the RNA foci or for the accumulation of MBNL1 within them.

8) Inhibition of pre-mRNA splicing causes MBNL1 to leave CUG^{exp} RNA foci.

It has been proposed that CUG^{exp} RNA foci form in DM1 cells as a result of the inefficient splicing and export from the nucleus of the DMPK transcripts that contain the expansion[26]. Spliceostatin A (SSA) is a potent inhibitor of pre-mRNA splicing, preventing the spliceosome transition from complex A to B and resulting in “freezing” of the spliceosome[29]. We have demonstrated, using DRB, that on-going transcription is not required for the maintenance of foci in DM1 cells, implying that their RNA core is highly stable. To investigate the effects of splicing inhibition on CUG^{exp} RNA foci formation and MBNL1 distribution in DM1 HLE cells, cells were treated with SSA, fixed and immunostained using anti MBNL1 in conjunction with FISH using a GAC_{10} probe (figure 8A). Analysis of the number of foci per nucleus (arrows in figure 8A) shows no significant difference in the number of foci after 24hrs of splicing inhibition (figure 8B). However, the foci were less distinct when visualized either using the GAC_{10} probe, or anti-MBNL1 signal. To investigate this further, we quantified the amount of MBNL1 within foci in SSA inhibited and uninhibited cells. The accumulation of endogenous MBNL1 in the CUGexp RNA foci was significantly reduced after 24hrs of SSA inhibition

(figure 8C). To visualize this more directly, DM1 patient cells expressing GFP-MBNL1 were imaged by time-lapse microscopy during SSA inhibition (fig 8D). Before addition of the inhibitor, clear GFP-MBNL1 foci were observed (arrows). These foci, although still present after 4 hours of inhibition, were less easy to discern against the rest of the nuclear signal, consistent with the results in fixed cells showing a decrease in MBNL1 accumulation in foci following inhibition of splicing with SSA. Although expression of excess MBNL1 tends to result in an increased nucleoplasmic pool, rather than increased accumulation into CUG^{exp} foci (figure 5), it is important to establish that the amount of MBNL1 protein is not affected by inhibition of splicing. Western blot analysis (figure 8E) confirmed no significant alteration in MBNL1 protein levels when normalized against the nuclear protein, coilin (Student's unpaired T test P=0.8820, n=2).

Discussion

A minor proportion of MBNL1 accumulates in CUG^{exp} RNA foci in lens epithelial cells

DM1 has a complex pathology, affecting many different tissue types. Of the many symptoms observed, the presence of cataracts is the most prevalent and sometimes the only symptom seen. This makes lens epithelial cells a particularly appropriate model to investigate cellular changes associated with DM1. Although the molecular pathology of DM1 is not well understood, the basic genetic defect is the presence of an expanded CTG repeat in the DMPK1 gene, leading to the formation of pre-mRNA foci containing CUG repeats in the nucleus of the cell (CUG^{exp} RNA foci). These repeats accumulate the MBNL1 protein, an important alternative splicing factor that has recently also been implicated in the localization of mature mRNAs in the cytoplasm [8] and in regulation of mRNA decay[30]. It is proposed that the accumulation of MBNL1 in nuclear CUG^{exp} RNA foci results in sufficient sequestration of nuclear MBNL1 to disrupt its normal function in regulating complex patterns of alternative splicing, resulting in aberrant splicing of a number of transcripts and ultimately leading to DM1 pathology[31-33]. We have demonstrated here the presence of CUG^{exp} RNA foci in the nuclei of lens epithelial cells from DM1 patients and the accumulation of MBNL1 protein in these foci. Defects in the epithelial layer of the lens can lead to cataract both during development and in the mature lens [34]. The presence of CUGexp RNA foci in the epithelial cells of DM1 patients could therefore explain the strong association of cataract with DM1. However, the proportion of total cellular MBNL1 in the CUG^{exp} RNA foci is extremely small (0.5% for endogenous MBNL1), so it is difficult to rationalize how this can cause sufficient loss of function of nuclear MBNL1 to result in aberrant splicing and consequent downstream pathology. While studies have demonstrated that defects in RNA splicing increase with increasing MBNL1 depletion [35], no splicing defects were detected until 67% of total endogenous MBNL1 was lost.

MBNL1 has a complex and highly dynamic cellular distribution in the lens epithelium, correlating to transcriptional activity

Endogenous and GFP-tagged MBNL1 localize to both the nucleus and the cytoplasm in lens epithelial cells grown in culture. The majority of cells show MBNL1 diffusely localized with a noticeable enrichment in the nucleus compared to the cytoplasm and an exclusion from the nucleolus. A smaller proportion of cells show clear co-localization of MBNL1 with nuclear speckles containing splicing factors. Accumulation in splicing speckles is characteristic of many splicing factors, with the speckles thought to serve as a reservoir from which they are recruited to participate in splicing at sites of transcription when required[25]. The diffuse localization of MBNL1, while uncharacteristic for a pre mRNA splicing factor, is similar to the distribution seen for snRNP proteins associated with the minor U11/12 spliceosome, present at 1/100th the amount of the major spliceosome [36-39] . Interestingly, disturbances in the cellular repertoire of minor splicesomal snRNPs have been implicated in widespread splicing defects associated with another neurodegenerative condition, Spinal Muscular Atrophy [40-42] . The largely diffuse nuclear localization of MBNL1 suggests that the protein is not present in excess within the nucleus and that most of the MBNL1 present is actively involved in pre-mRNA splicing. It is conceivable, if the role of MBNL1 in splicing is in

constant demand in these cells, that even the tiny amount localized to CUG^{exp} RNA foci may represent a sufficient loss to result in altered splicing patterns. A still smaller proportion of HLE cells show little nuclear MBNL1 with most of the protein present in the cytoplasm. These cells appear to have lower levels of transcription compared to the rest of the population.

The use of the global inhibitor of transcription, DRB, results in a marked loss of MBNL1 from the nucleus and its migration into the cytoplasm, leaving some MBNL1 sequestered by the RNA foci in DM1 cell lines. While this is a distinct contrast to the behavior of well-studied splicing factors such as SC-35 and ASF/SF2 that migrate to rounded-up speckles in transcriptionally inhibited cells[27, 28], it may well reflect the diverse roles proposed for MBNL1 in cellular RNA metabolism. MBNL1 has recently been implicated in mRNA decay [30] and in the sub-cellular localization of mature mRNAs, particularly those associated with cellular membranes and synapses[8]. In transcriptionally inhibited cells, the nuclear role for MBNL1 in splicing will be redundant, but its roles in other areas of RNA metabolism will persist. Long-lived mRNAs have been documented in lens fibre cells even after the elimination of the cell nucleus [43, 44]. The marked differences seen in sub-cellular localization of MBNL1 in the intact lens indicate that these different sub-cellular distributions, related to transcriptional activity, are of physiological relevance. Indeed, the dynamic re-distribution of MBNL1 between the nucleus and the cytoplasm during programmes of cellular differentiation in the lens epithelium or early fibre cells may be the key process that is compromised in DM1. Minor disruptions can have profound consequences in the lens since it has little opportunity to repair or recover from defects in its highly ordered programme of differentiation. The Drosophila homolog of MBNL1, muscleblind, was originally isolated as a gene required for photoreceptor differentiation[45], while MBNL proteins have been demonstrated to be developmentally regulated in the chick retina[46]. Recent RNA sequencing data has implicated MBNL proteins as key negative regulators of transcriptional pathways involved in the maintenance of pluripotency in embryonic stem cells, with over-expression of MBNL proteins promoting alternative splicing patterns associated with differentiated cells[11]. We see MBNL1 localized to the cytoplasm in regions of the lens epithelium implicated as the location of a stem cell-like population, with a marked relocalization to the nucleus seen as cells differentiate into fibre cells and migrate towards the centre of the lens. These data suggest that the sub-cellular distribution of MBNL1, as well as its absolute expression level, may be of importance for its regulatory roles in mRNA metabolism.

The lens as a model for DM1

As a model system for the study of the mechanisms that lead to DM1 the lens and lens cells from patients presents a unique opportunity. Whether findings in the lens can be extrapolated to other tissues remains to be seen. Rapid exchange of GFP-MBNL1 within CUG^{exp} foci has, however, also been documented in DM1 patient fibroblasts [14] and in a mouse myoblast model expressing CUG-repeat RNA [47], suggesting that results obtained in lens cells may be representative of other tissues. The lens is the first tissue to present the DM1 phenotype, as cataracts, in patients. The lens is known to be extremely sensitive to many forms of insult including ultra violet light, glycation, oxidation and the ageing process, because it is unable easily to replace and repair damaged cells [34]. Indeed the lens is rich in mechanisms to resist these insults

including small-heat-shock protein chaperones and high levels of glutathione [48-51]. It may be that the high levels of transcriptional activity required to produce the crystallins and other proteins necessary for fibre cell differentiation makes lens epithelial cells exquisitely sensitive to very small disturbances in the relative levels of different splicing components. Alternatively disruption of the epithelium caused by splicing abnormalities may lead to problems with the homeostasis of the underlying fibre cells or defects in fibre cells differentiation that present later in mature fibre cells. Either a small reduction of available nuclear MBNL1, or the inappropriate retention of small amounts of MBNL1 within the nucleus during transcriptional shut-down could result in such subtle disturbances. To address the balance of alternative splicing factors in lens epithelial cells, we are currently investigating the expression and localization of the protein CUG-BP1, which is known to act antagonistically with MBNL1 during muscle heart development and, like MBNL1, also has wider roles in mRNA metabolism [52].

We have demonstrated relocalization of MBNL1 from the nucleus to the cytoplasm both on transcriptional inhibition in cell lines and during programmed fibre cell differentiation in intact lenses. In addition to its role in alternative splice site selection, MBNL1 has recently been implicated in chaperoning mature mRNAs and determining their sub-cellular localization [8]. It may be disturbances in these functions, rather than splicing, caused by inappropriate retention of MBNL1 by CUG^{exp} foci in the nucleus, that result in cellular disfunction. Whichever model proves to be correct, the unique sensitivity of the lens in DM1 and its propensity to form cataracts will allow experimenters to identify subtle changes in cellular metabolism that lead to the DM1 phenotype.

CUG^{exp} RNA foci do not require on-going transcription for their maintenance but are sensitive to inhibition of splicing

The DMPK RNA that forms nuclear foci in DM1 is both polyadenylated and spliced [2, 26]. These processing events are required for exit of mRNA from the nucleus under normal circumstances. The reason for the failure of mRNA containing expanded CUG repeats to exit the nucleus is not fully understood but it has been proposed that the mRNA is blocked at an early stage of nuclear export at the periphery of splicing speckles[26]. The association of RNA transcripts within the foci with MBNL1 is unlikely to result in inhibition of the proposed export pathway via speckles as we have demonstrated that MBNL1 is able to enter and leave speckles. Inhibition of the export of DMPK RNA containing CUG expansions is, therefore, likely to be by a mechanism other than its association with MBNL1. While the tendency of CUG^{exp} RNA foci to associate with speckles has been reported[10, 26], our time-lapse studies suggest that this association is not as static as previously inferred, with at least some of the foci able to dissociate from speckles and move within the nucleus. The foci in lens epithelial cells were unaffected by inhibition of transcription using DRB, with both the RNA core and the sequestered MBNL1 protein remaining in the absence of on-going transcription. This level of stability is consistent with that seen in DM1 fibroblasts, where the half-life of RNA in the foci was estimated to be 15hr following transcriptional inhibition with actinomycin D[2]. In contrast to this, the use of spliceostatin A (SSA) to inhibit pre-mRNA splicing directly did not result in the loss of MBNL1 from the nucleus, but did cause a statistically significant decrease in the proportion of nuclear MBNL1

sequestered into foci. SSA inhibits splicing by targeting SF3b, a multimeric protein component of the U2 snRNP and blocking the transition from the A to the B spliceosomal complex[29, 53]. The presence of these 'stalled' spliceosomes may account for the retention of MBNL1 in the nucleus. It is not clear whether the loss of MBNL1 from foci is associated with shrinkage of the foci themselves. Visual inspection of RNA in situ hybridizations using GAC10 DNA probes suggests that the RNA foci are smaller and less bright, but accurate quantitation of this result is not possible due to the absence of a genuine RNA signal elsewhere in the cell. SSA has been demonstrated to enable the leakage of improperly processed pre-mRNA into the cytoplasm, although the mechanism for this is not understood[54]. It is possible that SSA treatment of DM1 lens epithelial cells relieves the block on the export of the CUG repeat-containing DMPK1 RNA. Whether the RNA cores of the foci are decreased by SSA or not, the sequestration of MBNL1 into the foci is reduced. Since SSA and other inhibitors of pre-mRNA splicing [53-57] are currently under investigation as anti-cancer drugs, these results raise the possibility that such compounds may also be of benefit as therapies for DM1.

Acknowledgements
The authors would like to thank Calum Thomson for help with sectioning porcine lenses; Prof. G. Morris (RJAH Orthopaedic Hospital, Oswestry, UK) for MBNL1 antibodies; Prof. T. Cooper (Baylor College of Medicine, Houston, TX) for pGFP-MBNL1; Prof. A. Lamond (University of Dundee, UK) for pmCherry-SC35 and pmCherry-ASF and Prof. J. Lippincott-Schwartz (NIH, Bethesda, MD) for the cDNA for PAGFP and Prof. M. Yoshida (RIKEN, Japan) for Spliceostatin A. The authors declare no conflicts of interest.

Funding
SMC was funded by a PhD studentship from the Scottish Universities Life Science Alliance (SULSA) and the Biotechnology and Biological Sciences Research Council (BBSRC).

REFERENCES

1 Brook, J. D., McCurrach, M. E., Harley, H. G., Buckler, A. J., Church, D., Aburatani, H., Hunter, K., Stanton, V. P., Thirion, J. P., Hudson, T. and et al. (1992) Molecular basis of myotonic dystrophy: expansion of a trinucleotide (CTG) repeat at the 3' end of a transcript encoding a protein kinase family member. Cell. **69**, 385

2 Davis, B. M., McCurrach, M. E., Taneja, K. L., Singer, R. H. and Housman, D. E. (1997) Expansion of a CUG trinucleotide repeat in the 3' untranslated region of myotonic dystrophy protein kinase transcripts results in nuclear retention of transcripts. P Natl Acad Sci USA. **94**, 7388-7393

3 Taneja, K. L., McCurrach, M., Schalling, M., Housman, D. and Singer, R. H. (1995) Foci of trinucleotide repeat transcripts in nuclei of myotonic dystrophy cells and tissues. J Cell Biol. **128**, 995-1002

4 Ho, T. H., Charlet, B. N., Poulos, M. G., Singh, G., Swanson, M. S. and Cooper, T. A. (2004) Muscleblind proteins regulate alternative splicing. EMBO J. **23**, 3103-3112

5 Sen, S., Talukdar, I., Liu, Y., Tam, J., Reddy, S. and Webster, N. J. (2010) Muscleblind-like 1 (Mbnl1) promotes insulin receptor exon 11 inclusion via binding to a downstream evolutionarily conserved intronic enhancer. J Biol Chem. **285**, 25426-25437

6 Mankodi, A., Urbinati, C. R., Yuan, Q. P., Moxley, R. T., Sansone, V., Krym, M., Henderson, D., Schalling, M., Swanson, M. S. and Thornton, C. A. (2001) Muscleblind localizes to nuclear foci of aberrant RNA in myotonic dystrophy types 1 and 2. Hum Mol Genet. **10**, 2165-2170

7 Onishi, H., Kino, Y., Morita, T., Futai, E., Sasagawa, N. and Ishiura, S. (2008) MBNL1 associates with YB-1 in cytoplasmic stress granules. J Neurosci Res. **86**, 1994-2002

8 Wang, E. T., Cody, N. A., Jog, S., Biancolella, M., Wang, T. T., Treacy, D. J., Luo, S., Schroth, G. P., Housman, D. E., Reddy, S., Lecuyer, E. and Burge, C. B. (2012) Transcriptome-wide regulation of pre-mRNA splicing and mRNA localization by muscleblind proteins. Cell. **150**, 710-724

9 Lin, X., Miller, J. W., Mankodi, A., Kanadia, R. N., Yuan, Y., Moxley, R. T., Swanson, M. S. and Thornton, C. A. (2006) Failure of MBNL1-dependent post-natal splicing transitions in myotonic dystrophy. Hum Mol Genet. **15**, 2087-2097

10 Holt, I., Mittal, S., Furling, D., Butler-Browne, G. S., Brook, J. D. and Morris, G. E. (2007) Defective mRNA in myotonic dystrophy accumulates at the periphery of nuclear splicing speckles. Genes Cells. **12**, 1035-1048

11 Han, H., Irimia, M., Ross, P. J., Sung, H. K., Alipanahi, B., David, L., Golipour, A., Gabut, M., Michael, I. P., Nachman, E. N., Wang, E., Trcka, D., Thompson, T., O'Hanlon, D., Slobodeniuc, V., Barbosa-Morais, N. L., Burge, C. B., Moffat, J., Frey, B. J., Nagy, A., Ellis, J., Wrana, J. L. and Blencowe, B. J. (2013) MBNL proteins repress ES-cell-specific alternative splicing and reprogramming. Nature. **498**, 241-245

12 Kidd, A., Turnpenny, P., Kelly, K., Clark, C., Church, W., Hutchinson, C., Dean, J. C. and Haites, N. E. (1995) Ascertainment of myotonic dystrophy through cataract by selective screening. J Med Genet. **32**, 519-523

13 Liquori, C. L., Ricker, K., Moseley, M. L., Jacobsen, J. F., Kress, W., Naylor, S. L., Day, J. W. and Ranum, L. P. (2001) Myotonic dystrophy type 2 caused by a CCTG expansion in intron 1 of ZNF9. Science. **293**, 864-867

14 Ho, T. H., Savkur, R. S., Poulos, M. G., Mancini, M. A., Swanson, M. S. and Cooper, T. A. (2005) Colocalization of muscleblind with RNA foci is separable from mis-regulation of alternative splicing in myotonic dystrophy. J Cell Sci. **118**, 2923-2933

15 Wride, M. A. (2011) Lens fibre cell differentiation and organelle loss: many paths lead to clarity. Philos Trans R Soc Lond B Biol Sci. **366**, 1219-1233

16 Dahm, R., Gribbon, C., Quinlan, R. A. and Prescott, A. R. (1998) Changes in the nucleolar and coiled body compartments precede lamina and chromatin reorganization during fibre cell denucleation in the bovine lens. Eur J Cell Biol. **75**, 237-246
17 Dahm, R., Procter, J. E., Ireland, M. E., Lo, W. K., Mogensen, M. M., Quinlan, R. A. and Prescott, A. R. (2007) Reorganization of centrosomal marker proteins coincides with epithelial cell differentiation in the vertebrate lens. Exp Eye Res. **85**, 696-713
18 Gribbon, C., Dahm, R., Prescott, A. R. and Quinlan, R. A. (2002) Association of the nuclear matrix component NuMA with the Cajal body and nuclear speckle compartments during transitions in transcriptional activity in lens cell differentiation. Eur J Cell Biol. **81**, 557-566
19 Rhodes, J. D., Monckton, D. G., McAbney, J. P., Prescott, A. R. and Duncan, G. (2006) Increased SK3 expression in DM1 lens cells leads to impaired growth through a greater calcium-induced fragility. Human Molecular Genetics. **15**, 3559-3568
20 Ellis, J. D., Lleres, D., Denegri, M., Lamond, A. I. and Caceres, J. F. (2008) Spatial mapping of splicing factor complexes involved in exon and intron definition. The Journal of cell biology. **181**, 921-934
21 Patterson, G. H. and Lippincott-Schwartz, J. (2002) A photoactivatable GFP for selective photolabeling of proteins and cells. Science. **297**, 1873-1877
22 Sleeman, J. E., Trinkle-Mulcahy, L., Prescott, A. R., Ogg, S. C. and Lamond, A. I. (2003) Cajal body proteins SMN and Coilin show differential dynamic behaviour in vivo. Journal of cell science. **116**, 2039-2050
23 Kambach, C. and Mattaj, I. W. (1992) Intracellular distribution of the U1A protein depends on active transport and nuclear binding to U1 snRNA. The Journal of cell biology. **118**, 11-21
24 Kalsotra, A., Xiao, X. S., Ward, A. J., Castle, J. C., Johnson, J. M., Burge, C. B. and Cooper, T. A. (2008) A postnatal switch of CELF and MBNL proteins reprograms alternative splicing in the developing heart. P Natl Acad Sci USA. **105**, 20333-20338
25 Spector, D. L. and Lamond, A. I. (2011) Nuclear speckles. Cold Spring Harb Perspect Biol. **3**
26 Smith, K. P., Byron, M., Johnson, C., Xing, Y. and Lawrence, J. B. (2007) Defining early steps in mRNA transport: mutant mRNA in myotonic dystrophy type I is blocked at entry into SC-35 domains. Journal of Cell Biology. **178**, 951-964
27 Carmo-Fonseca, M., Pepperkok, R., Carvalho, M. T. and Lamond, A. I. (1992) Transcription-dependent colocalization of the U1, U2, U4/U6, and U5 snRNPs in coiled bodies. The Journal of cell biology. **117**, 1-14
28 Spector, D. L., O'Keefe, R. T. and Jimenez-Garcia, L. F. (1993) Dynamics of transcription and pre-mRNA splicing within the mammalian cell nucleus. Cold Spring Harb Symp Quant Biol. **58**, 799-805
29 Roybal, G. A. and Jurica, M. S. (2010) Spliceostatin A inhibits spliceosome assembly subsequent to prespliceosome formation. Nucleic acids research. **38**, 6664-6672
30 Masuda, A., Andersen, H. S., Doktor, T. K., Okamoto, T., Ito, M., Andresen, B. S. and Ohno, K. (2012) CUGBP1 and MBNL1 preferentially bind to 3' UTRs and facilitate mRNA decay. Sci Rep. **2**, 209
31 Miller, J. W., Urbinati, C. R., Teng-Umnuay, P., Stenberg, M. G., Byrne, B. J., Thornton, C. A. and Swanson, M. S. (2000) Recruitment of human muscleblind proteins to (CUG)(n) expansions associated with myotonic dystrophy. The EMBO journal. **19**, 4439-4448
32 Osborne, R. J. and Thornton, C. A. (2006) RNA-dominant diseases. Human molecular genetics. **15 Spec No 2**, R162-169

33 Philips, A. V., Timchenko, L. T. and Cooper, T. A. (1998) Disruption of splicing regulated by a CUG-binding protein in myotonic dystrophy. Science. **280**, 737-741
34 Hightower, K. R. (1995) The role of the lens epithelium in development of UV cataract. Curr Eye Res. **14**, 71-78
35 Jog, S. P., Paul, S., Dansithong, W., Tring, S., Comai, L. and Reddy, S. (2012) RNA splicing is responsive to MBNL1 dose. PLoS One. **7**, e48825
36 Clelland, A. K., Bales, A. B. and Sleeman, J. E. (2012) Changes in intranuclear mobility of mature snRNPs provide a mechanism for splicing defects in spinal muscular atrophy. Journal of cell science. **125**, 2626-2637
37 Lorkovic, Z. J., Lehner, R., Forstner, C. and Barta, A. (2005) Evolutionary conservation of minor U12-type spliceosome between plants and humans. Rna. **11**, 1095-1107
38 Wang, H., Gao, M. X., Li, L., Wang, B., Hori, N. and Sato, K. (2007) Isolation, expression, and characterization of the human ZCRB1 gene mapped to 12q12. Genomics. **89**, 59-69
39 Zhao, E., Li, J., Xie, Y., Jin, W., Zhang, Z., Chen, J., Zeng, L., Yin, G., Qian, J., Wu, H., Ying, K., Zhao, R. C. and Mao, Y. (2003) Cloning and identification of a novel human RNPC3 gene that encodes a protein with two RRM domains and is expressed in the cell nucleus. Biochem Genet. **41**, 315-323
40 Gabanella, F., Butchbach, M. E., Saieva, L., Carissimi, C., Burghes, A. H. and Pellizzoni, L. (2007) Ribonucleoprotein assembly defects correlate with spinal muscular atrophy severity and preferentially affect a subset of spliceosomal snRNPs. PLoS One. **2**, e921
41 Sleeman, J. E. (2013) snRNPs and mRNPs: linking RNA processing and transport to Spinal Muscular Atrophy. Biochem Soc Trans. **41**
42 Zhang, Z., Lotti, F., Dittmar, K., Younis, I., Wan, L., Kasim, M. and Dreyfuss, G. (2008) SMN deficiency causes tissue-specific perturbations in the repertoire of snRNAs and widespread defects in splicing. Cell. **133**, 585-600
43 Laurent, M., Romquin, N., Counis, M. F., Muel, A. S. and Courtois, Y. (1987) Collagen synthesis by long-lived mRNA in embryonic chicken lens. Dev Biol. **121**, 166-173
44 Reeder, R. and Bell, E. (1965) Short- and long-lived messenger RNA in embryonic chick lens. Science. **150**, 71-72
45 Begemann, G., Paricio, N., Artero, R., Kiss, I., Perez-Alonso, M. and Mlodzik, M. (1997) muscleblind, a gene required for photoreceptor differentiation in Drosophila, encodes novel nuclear Cys3His-type zinc-finger-containing proteins. Development. **124**, 4321-4331
46 Huang, H., Wahlin, K. J., McNally, M., Irving, N. D. and Adler, R. (2008) Developmental regulation of muscleblind-like (MBNL) gene expression in the chicken embryo retina. Dev Dyn. **237**, 286-296
47 Querido, E., Gallardo, F., Beaudoin, M., Menard, C. and Chartrand, P. (2011) Stochastic and reversible aggregation of mRNA with expanded CUG-triplet repeats. Journal of cell science. **124**, 1703-1714
48 Giblin, F. J. (2000) Glutathione: a vital lens antioxidant. J Ocul Pharmacol Ther. **16**, 121-135
49 McGreal, R. S., Kantorow, W. L., Chauss, D. C., Wei, J., Brennan, L. A. and Kantorow, M. (2012) alphaB-crystallin/sHSP protects cytochrome c and mitochondrial function against oxidative stress in lens and retinal cells. Biochim Biophys Acta. **1820**, 921-930
50 Mesa, R. and Bassnett, S. (2013) UV-B-Induced DNA Damage and Repair in the Mouse Lens. Investigative ophthalmology & visual science. **54**, 6789-6797

51 Umapathy, A., Donaldson, P. and Lim, J. (2013) Antioxidant Delivery Pathways in the Anterior Eye. Biomed Res Int. **2013**, 207250
52 Lee, J. E. and Cooper, T. A. (2009) Pathogenic mechanisms of myotonic dystrophy. Biochem Soc Trans. **37**, 1281-1286
53 Corrionero, A., Minana, B. and Valcarcel, J. (2011) Reduced fidelity of branch point recognition and alternative splicing induced by the anti-tumor drug spliceostatin A. Genes Dev. **25**, 445-459
54 Lo, C. W., Kaida, D., Nishimura, S., Matsuyama, A., Yashiroda, Y., Taoka, H., Ishigami, K., Watanabe, H., Nakajima, H., Tani, T., Horinouchi, S. and Yoshida, M. (2007) Inhibition of splicing and nuclear retention of pre-mRNA by spliceostatin A in fission yeast. Biochem Biophys Res Commun. **364**, 573-577
55 Furumai, R., Uchida, K., Komi, Y., Yoneyama, M., Ishigami, K., Watanabe, H., Kojima, S. and Yoshida, M. (2010) Spliceostatin A blocks angiogenesis by inhibiting global gene expression including VEGF. Cancer Sci. **101**, 2483-2489
56 Kaida, D., Motoyoshi, H., Tashiro, E., Nojima, T., Hagiwara, M., Ishigami, K., Watanabe, H., Kitahara, T., Yoshida, T., Nakajima, H., Tani, T., Horinouchi, S. and Yoshida, M. (2007) Spliceostatin A targets SF3b and inhibits both splicing and nuclear retention of pre-mRNA. Nat Chem Biol. **3**, 576-583
57 Kotake, Y., Sagane, K., Owa, T., Mimori-Kiyosue, Y., Shimizu, H., Uesugi, M., Ishihama, Y., Iwata, M. and Mizui, Y. (2007) Splicing factor SF3b as a target of the antitumor natural product pladienolide. Nat Chem Biol. **3**, 570-575

Figure legends

Figure 1) CUG^{exp} foci form in DM1 patient HLE cells and co-localize with endogenous and GFP-tagged MBNL1.
A) Simultaneous detection of MBNL1 using anti MBNL1 (green) and CUG^{exp} mRNA foci by in-situ hybridization using a GAC_{10} DNA probe (red) demonstrates co-localixation of MBNL1 protein and RNA foci in DM1 cells (yellow on merged image). The smaller panels are detailed views of the regions marked in the main panels.
B) In-situ hybridization using a GAC_{10} DNA probe (red) in DM1 cells expressing GFP-MBNL1 (green) demonstrates accumulation of GFP-MBNL1 in CUG^{exp} mRNA foci.
C) and D) No CUG^{exp} mRNA foci or characteristic punctate accumulations of endogenous MBNL1 (C) or GFP-MBNL1 (D) are seen in control HLE cells. Images are maximum intensity projections of deconvolved 0.2μm Z-sections. Bars on main panels= 20μm, on detailed panels= 5μm.
E) Graphical representation of the number of foci detected using anti MBNL1 antibody, GFP-MBNL1 and GAC_{10} probe. There are no significant differences in the number of foci per cell nucleus between GFP-MBNL1, endogenous MBNL1 and GAC_{10} probe foci or between DM1 cell lines (one way ANOVA, $P>0.05$, n=75 for each variable).

Figure 2) MBNL1 has a complex sub-cellular localization in lens epithelial cells
A) Endogenous MBNL1 (i and iv, red on overlay) localizes to both the nucleus (stained with DAPI, ii and v, blue on overlay) and the cytoplasm in lens epithelial cells. MBNL1 is largely excluded from nucleoli (white arrows) and accumulates in speckle-like structures (arrowheads) in both control cells (i to iii) and DM1 cells (iv to vi). Bright. Punctate accumulations of MBNL1, corresponding to CUG^{exp} mRNA foci are seen only in DM1 cells (yellow arrows). Images are single deconvolved z-sections. Bar=10μm.
B) Simultaneous detection of MBNL1 (i, green on overlay) and the snRNP protein U1A (ii, red on overlay) demonstrates co-localization of the two proteins in nuclear speckles (yellow/orange in iii). Images are maximum intensity projections of deconvolved 0.2μm Z-sections. Bar =20μm. The full 3D data-set (iv) was used to generate a cross section for intensity measurements (v) to confirm the co-localisation. vi) Scatter plot of pixel colocalization of U1A (red) and MBNL1 (green) gives Pearson's correlation coefficient =0.802.

Figure 3) MBNL1 moves between the nucleus and cytoplasm during lens development
A) Simultaneous detection of U1A and MBNL1 in transverse sections of porcine lenses shows that U1A (red) remains nuclear throughout lens cell differentiation. In contrast, MBNL1 (green) localizes to both the nucleus and cytoplasm in the anterior epithelium (top row), changing to a predominantly nuclear localization as cells enter the equatorial epithelium (middle row, arrows), remaining nuclear as cells begin to differentiate into cortical fibre cells (bottom row, arrowheads). DAPI staining (blue) shows the position of the nuclei. Images are maximum intensity projections of deconvolved 0.2μm Z-sections. Bar=10μm (top and middle rows), 25μm (bottom row).
B) Higher resolution imaging of differentiating fibre cells in transverse sections of porcine lenses demonstrate partial co-localization of U1A (i and red in v) and MBNL1 (ii and green in v) in nuclear speckles (arrows). DAPI (iii and blue in v) shows the

position of the nuclei and phalloidin 568 (iv and white in v) marks the boundaries of the elongated fibre cells. Images are single deconvolved z-sections. Bar=10μm.

Figure 4) MBNL1 localizes to the cytoplasm in cells with low transcriptional activity.
Incubation of HLE cells with 1mM 5-ethynyl uridine for 2hrs allows simultaneous detection within the nucleus (DAPI, blue on overlays) of endogenous MBNL1 (green on overlays) and sites of RNA transcription (red on overlays). Transcriptional activity is detected both in the nucleoplasm and in nucleoli (yellow arrows). Imaging of adjacent cells displaying differing distributions of MBNL1 reveals similar levels of transcription in cells with diffuse nuclear MBNL1 or MBNL1 accumulated in splicing speckles (A, arrows denote speckles). Cells with little nuclear MBNL1 and cytoplasmic accumulations of MBNL1 (B, arrowheads denote cytoplasmic accumultions), however, show very low levels of transcriptional activity in the nucleoplasm and nucleoli compared to neighbouring cells. Images are single optical sections. Bar =10μm.

Figure 5) The proportion of cellular MBNL1 sequestered by nuclear RNA foci is small
A) Charts representing the proportion of endogenous and GFP-tagged MBNL1 in DM1 and control HLE cells, calculated using object identification algorithms in Volocity (Perkin Elmer). Cells were counter stained with Phalloidin 568 and DAPI to identify the boundary of the cell cytoplasm and nucleus respectively. CUG^{exp} mRNA foci were identified using MBNL1 intensity. Multiple MBNL1 foci intensities were summed, where appropriate, to give the total MBNL1 sequestered into foci. n=15 per cell line.
B) There is no significant difference in the % of endogenous nuclear MBNL1 or of GFP-tagged nuclear MBNL1 sequestered into foci between DM1 cell lines, (One way anova, $P>0.05$, n=20 per cell line). There is, however, a significant difference between the mean % of GFP-MBNL1 and endogenous MBNL1 sequestered ($P<0.05$). The mean proportion of endogenous nuclear MBNL1 and GFP-MBNL1 sequestered into foci was 0.5% and 0.1% respectively.

Figure 6) MBNL1 sequestered by foci, and the foci themselves, are mobile
A) MBNL1 sequestered by foci is dynamic. GFP-MBNL1 in nuclear foci in DM1 cells was photobleached using a 488nm laser at 100% power with a 0.5sec pulse and subsequent time-lapse imaging carried out to monitor recovery of unbleached GFP-MBNL1 into foci. Arrow indicates the focus targeted for photobleaching, boxed region shows an enlarged view of the bleached region. Images are single z-sections. Bar= 10μm. Plotting the normalized recovery rates against time reveals a mobile fraction of around 50% in each of the four cell lines analyzed (n=25).
B) MBNL1 can exchange between foci. PA-GFP-MBNL1 in foci in DM1 cells was activated using a 405nm laser at 100% power with a 0.5sec pulse and subsequent time-lapse imaging carried out to determine the ability of MBNL1 to migrate within the nucleus. White arrow and enlarged box indicate the activated focus, red arrow and enlarged box indicate a different focus in the same nucleus. Migration of activated PA-GFPMBNL1 from the activated focus (white arrow) to the neighboring focus (red arrow) is clearly seen. Images are single z-sections. Bar= 10μm. Plotting of the fluorescence intensity of the activated focus (black squares) and the neighboring focus (red triangles) against time demonstrates the rapidity of the exchange. Representative data from experiments on 3 cells from each of the 4 DM1 HLE cell lines.
C) MBNL1 foci can move relative to nuclear speckles. Time-lapse imaging of DM1 cells

expressing both GFP-MBNL1 (top row and green on overlay) and mCherry-SC35 (red on overlay) demonstrates that, while some foci remain in close proximity to nuclear speckles over time (arrow), others are able to move more freely within the nucleus (arrowhead). Plotting the distance from the nearest speckle against time for individual foci shows the variety of movements seen. Images are maximum intensity projections of deconvolved 0.5μm Z-sections. Bar=10mm. Representative data from measurements of 18 individual foci in 4 separate cells. See also supplementary movie 1.

Figure 7) Experimental Inhibition of transcription does not affect the accumulation of MBNL1 in RNA foci, but causes migration of a large proportion of MBNL1 out of the nucleus .

A) RNA foci remain in transcriptionally inhibited cells. FISH using a GAC_{10} DNA probe in DM1 cells treated with the transcriptional inhibitor DRB reveals the persistence of RNA foci (red, arrows) over a 5 hour time course . The outline of the nucleus is shown by DAPI staining (blue). Images are maximum intensity projections of deconvolved 0.2μm Z-sections. Bar = 20μm,

B). Counts of the number of MBNL1 foci, detected using anti-MBNL1, in each cell nucleus in cells treated with DRB for 5 hours or untreated reveals no significant difference in the number MBNL1 foci per cell nucleus following DRB treatment. (one way ANOVA, $p>0.05$, n=25 per cell line, data presented as mean and SD).

C) MBNL1 is reversibly lost from the nucleus in transcriptionally inhibited cells. Time-lapse inaging of DM1 cells expressing GFP-MBNL1 and mCherry-ASF treated with 20μg/ml of DRB (left hand panel) shows gradual migration of GFP-MBNL1 out of the nucleus over a 5.5 hour period. Nuclear foci containing GFP-MBNL1 remain intact (arrows). mCherry-ASF shows the characteristic rounding up of nuclear speckles seen in transcriptionally inhibited cells. See also supplementary movie 2. Removal of DRB to reverse the transcriptional inhibition (right hand panel) shows the return of GFP-MBNL1 to the nucleus, and the reversal of the rounding up of mCherry-ASF speckles. Images are maximum intensity projections of deconvolved 0.2μm Z-sections. Bar=20μm. See also supplementary movie 3.

Figure 8) Inhibition of pre-mRNA splicing leaves the RNA core of the foci intact, but causes MBNL1 to leave the foci

A) RNA foci remain in cells inhibited for pre-mRNA splicing. Simultaneous FISH using a GAC_{10} DNA probe and immunodetection of endogenous MBNL1 in DM1 cells treated with the pre-mRNA splicing inhibitor SSA reveals the persistence of RNA foci (red, arrows) containing MBNL1 (green, arrows) over a 24 hour time course The outline of the nucleus is shown by DAPI staining (blue). The foci are visually less distinct in cells treated with SSA then in control cells (compare T=16hrs and T=24hrs with T=0). Bar = 20μm. Images are maximum intensity projections of deconvolved 0.2μm Z-sections.

B) Inhibition of splicing does not alter the number of foci per cell.
Counts of the number of foci per nucleus in DM1 HLE cells, detected using endogenous MBNL1 staining, show no significant difference in foci number between SSA inhibited and uninhibited DM1 HLE cells (Two tailed T test $P>0.05$, n=25 per cell line). Control cell lines showed no foci. Data are represented as mean and standard deviation.

C). Sequestration of MBNL1 into foci is decreased by inhibition of pre-mRNA splicing. The proportion of nuclear endogenous MBNL1 sequestered into foci in DM1 HLE cells treated with 25ng/ml Spliceostatin A (SSA) for 5hours shows a significant difference

compared to untreated DM1 HLE cells (Two tailed T-test $P<0.05$, n=25 per cell line.) Data are represented as mean and standard deviation).
D). Time-lapse imaging of DM1 HLE cells expressing GFPMBNL1 treated with 25ng/ml SSA shows that foci persist in cells inhibited for pre-mRNA splicing (arrows), but appear less distinct with time. Images are maximum intensity projections of deconvolved 0.5μm Z-sections. Bars= 20μm.
E) Western blot analysis of the expression of endogenous MBNL1 in cells treated with spliceostatin A for 16 hours shows no significant change compared to untreated cells using the nuclear protein, coilin, as a loading control (Student's unpaired T test, P=0.8820, n=2).

Figure 1

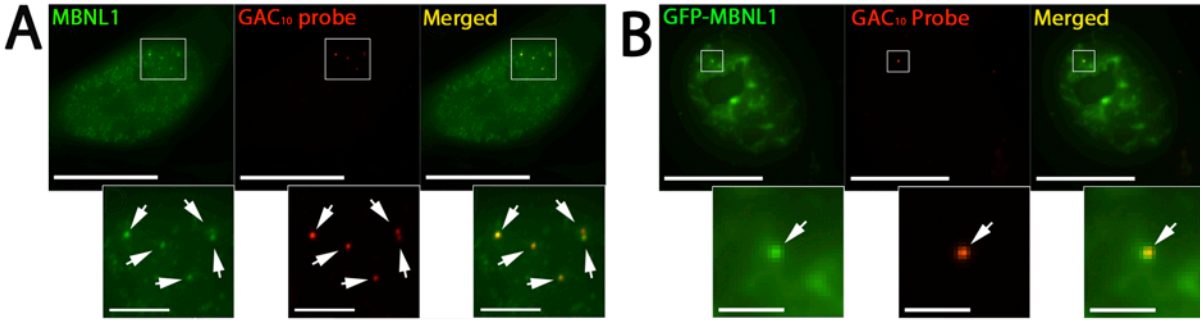
A
MBNL1
GAC10 probe
Merged
B
GFP-MBNL1
GAC10 Probe
Merged

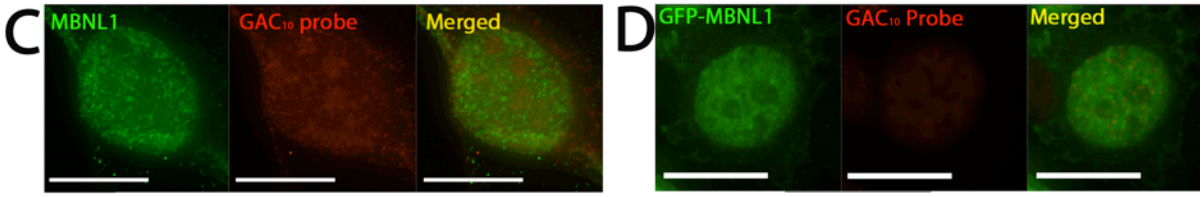
C
MBNL1
GAC10 probe
Merged
D
GFP-MBNL1
GAC10 Probe
Merged

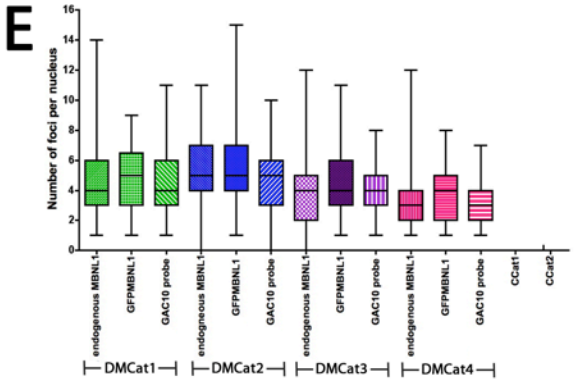
E
Number of foci per nucleus
endogenous MBNL1
GFPMBNL1
GAC10 probe
CCat1
CCat2
DMCat1
DMCat2
DMCat3
DMCat4

Figure 2

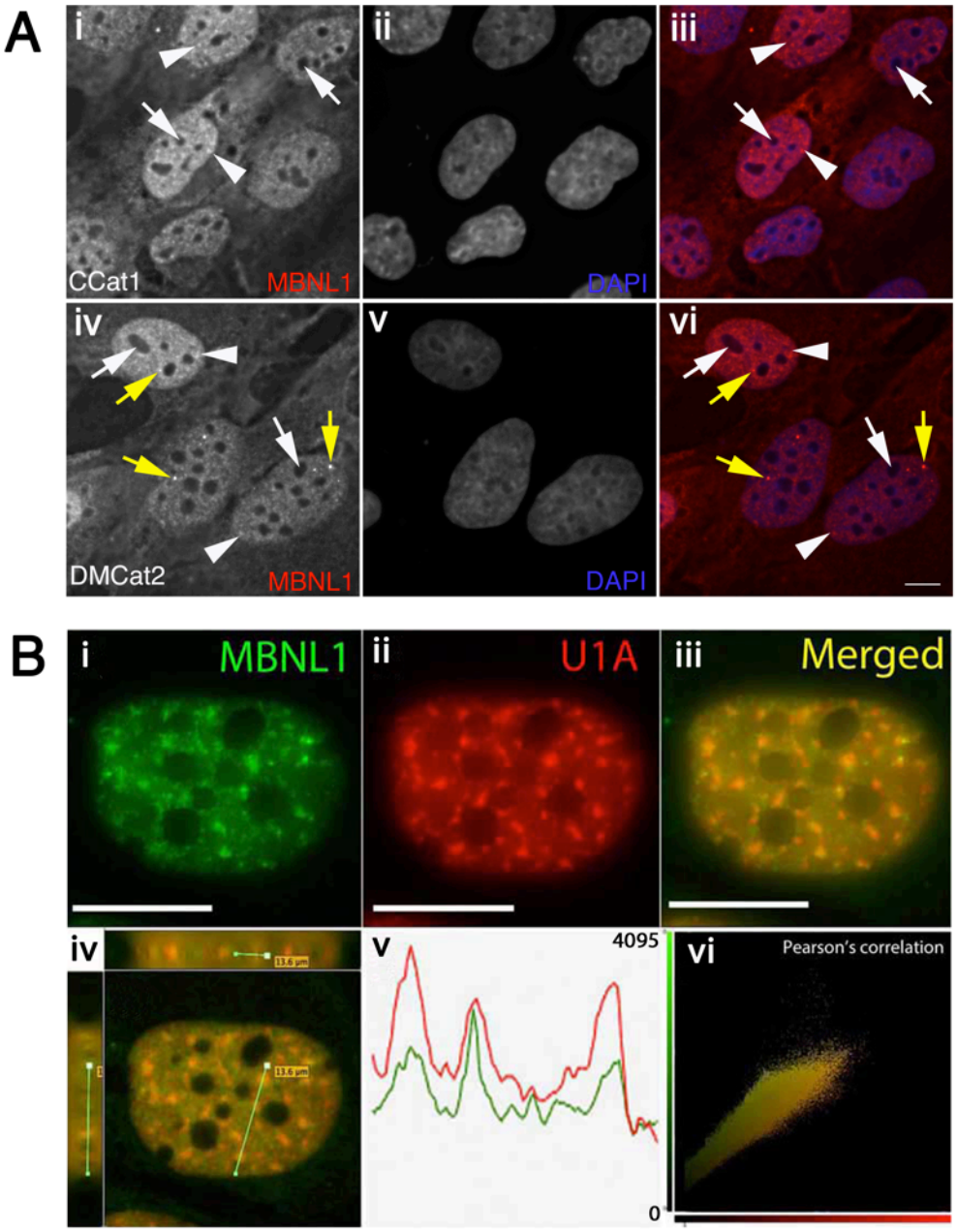
A
i
ii
iii
CCat1
MBNL1
DAPI
iv
v
vi
DMCat2
MBNL1
DAPI
B
i
MBNL1
ii
U1A
iii
Merged
iv
v
4095
0
vi
Pearson's correlation

Figure 3

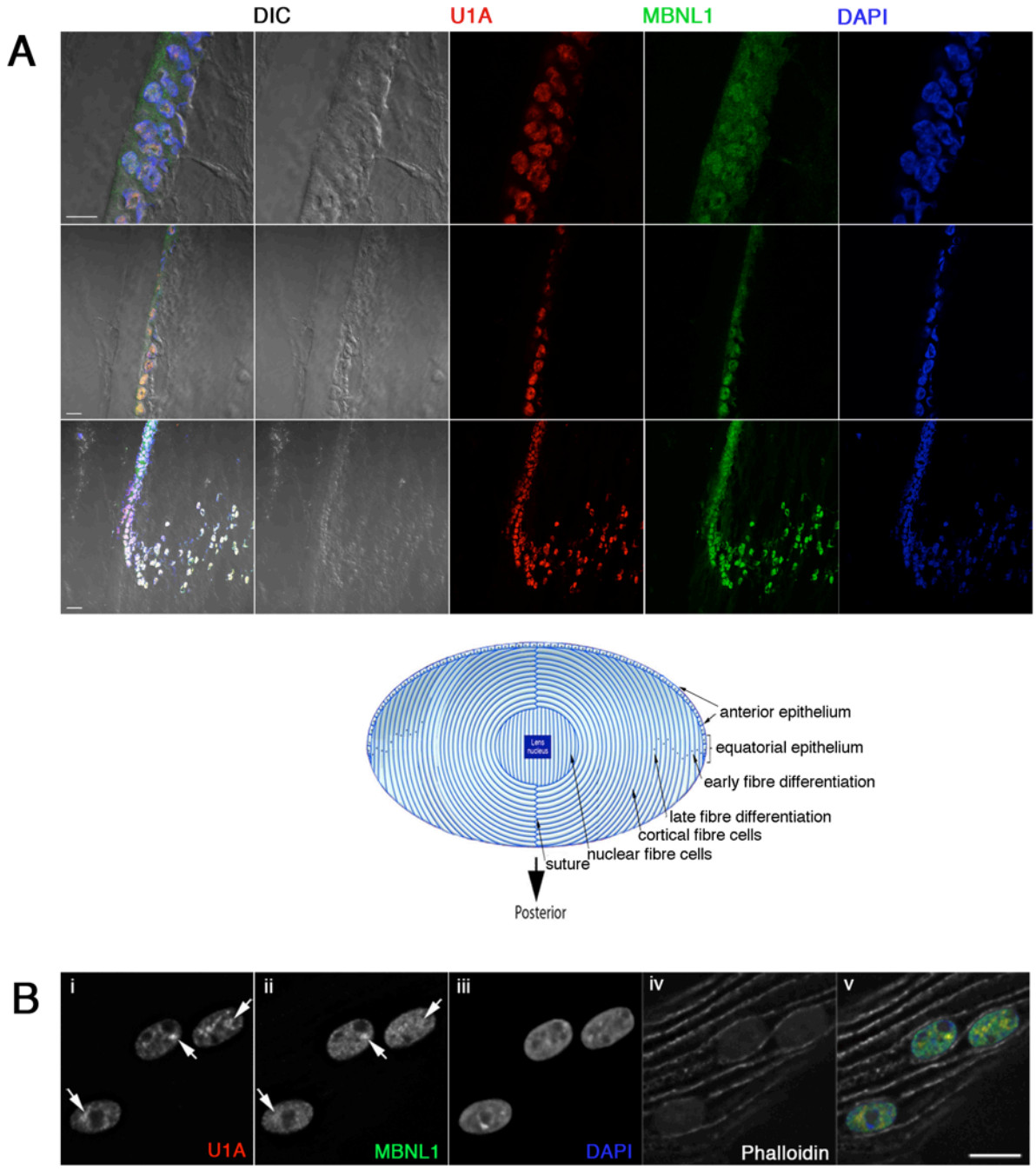
A
DIC
U1A
MBNL1
DAPI
anterior epithelium
equatorial epithelium
early fibre differentiation
late fibre differentiation
cortical fibre cells
nuclear fibre cells
suture
Posterior
B
i
ii
iii
iv
v
U1A
MBNL1
DAPI
Phalloidin

Figure 4

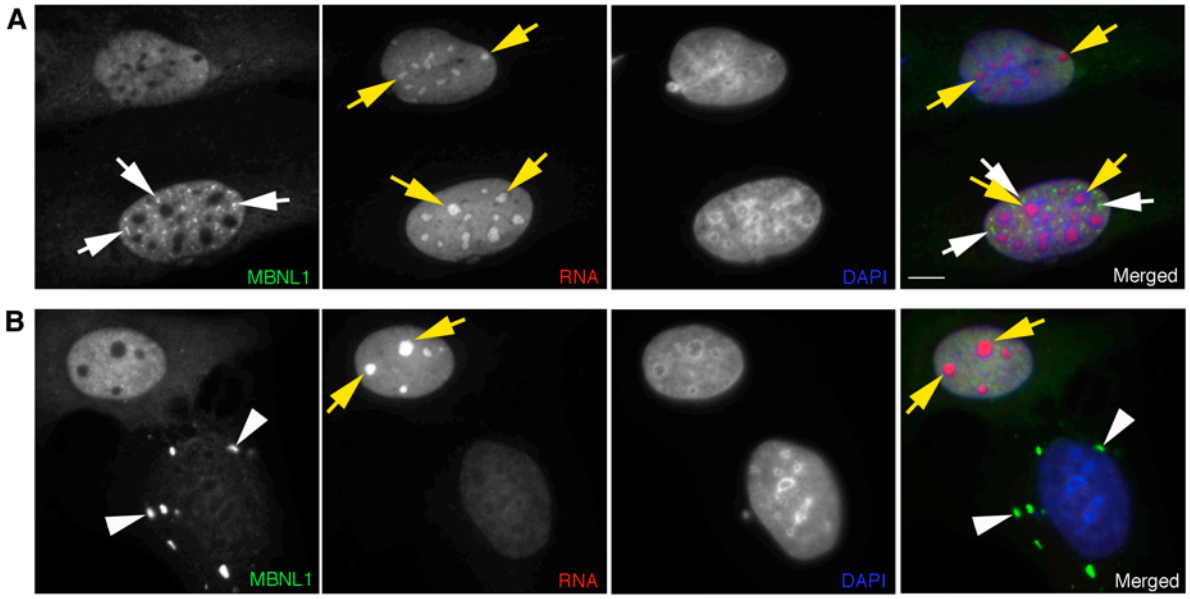

Figure 5

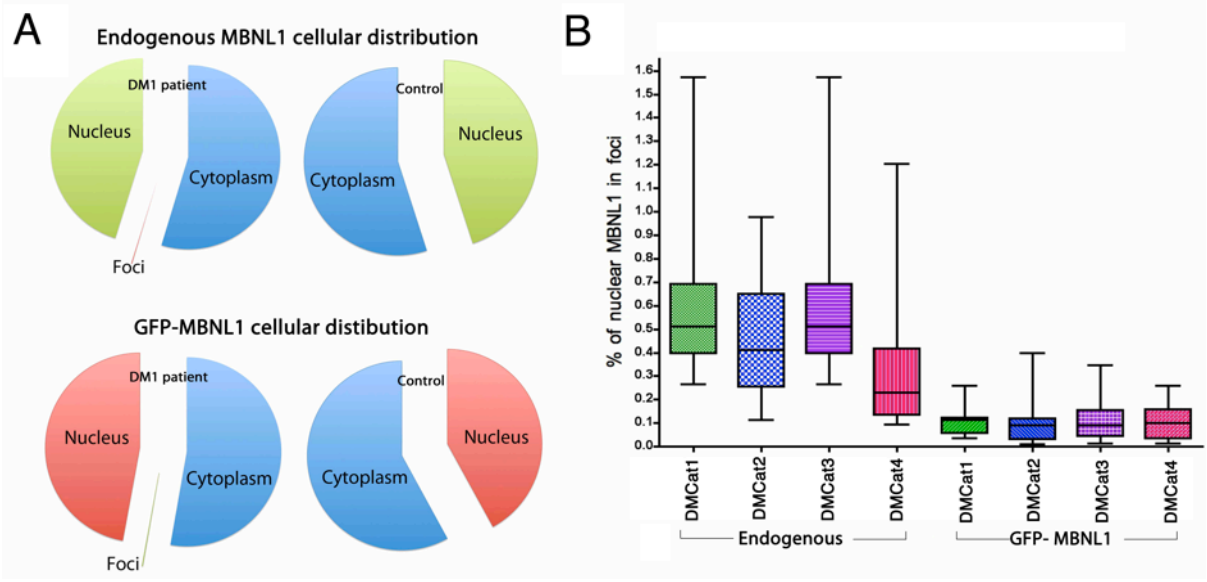

Figure 6

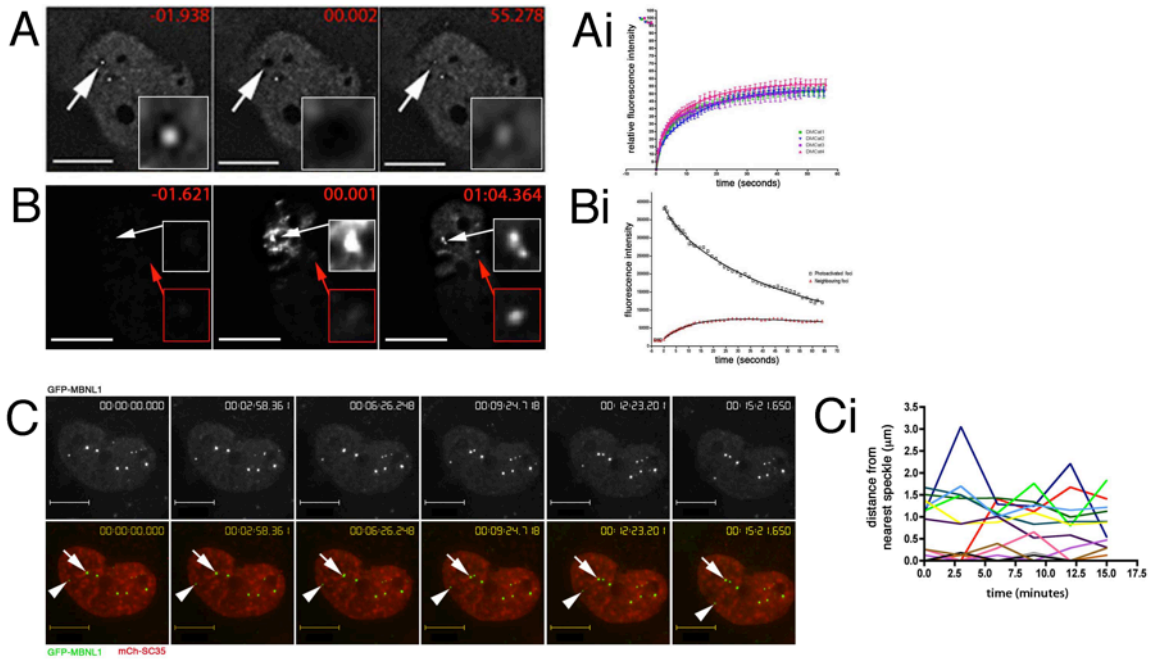
A
-01.938
00.002
55.278
Ai
relative fluorescence intensity
time (seconds)
B
-01.621
00.001
01:04.364
Bi
fluorescence intensity
time (seconds)
C
GFP-MBNL1
00:00:00.000
00:02:58.36 I
00:06:26.248
00:09:24.7 18
00: i2:23.20 I
00: i5:2 1.650
GFP-MBNL1
mCh-SC35
Ci
distance from nearest speckle (µm)
0.0
0.5
1.0
1.5
2.0
2.5
3.0
3.5
0.0
2.5
5.0
7.5
10.0
12.5
15.0
17.5
time (minutes)

Figure 7

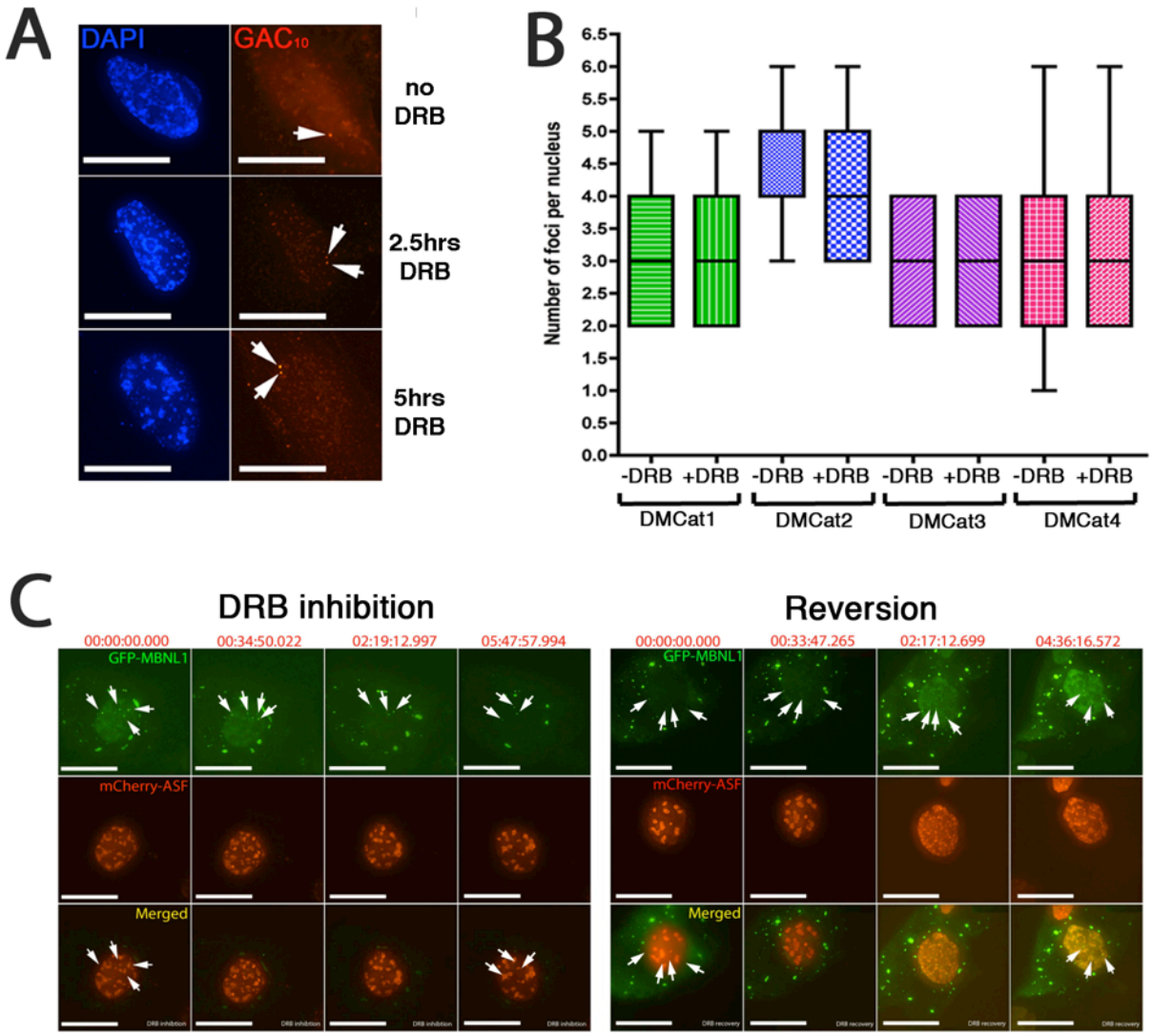
A
DAPI
GAC10
no DRB
2.5hrs DRB
5hrs DRB
B
Number of foci per nucleus
6.5
6.0
5.5
5.0
4.5
4.0
3.5
3.0
2.5
2.0
1.5
1.0
0.5
0.0
-DRB +DRB -DRB +DRB -DRB +DRB -DRB +DRB
DMCat1
DMCat2
DMCat3
DMCat4
C
DRB inhibition
Reversion
00:00:00.000
00:34:50.022
02:19:12.997
05:47:57.994
00:00:00.000
00:33:47.265
02:17:12.699
04:36:16.572
GFP-MBNL1
mCherry-ASF
Merged

Figure 8

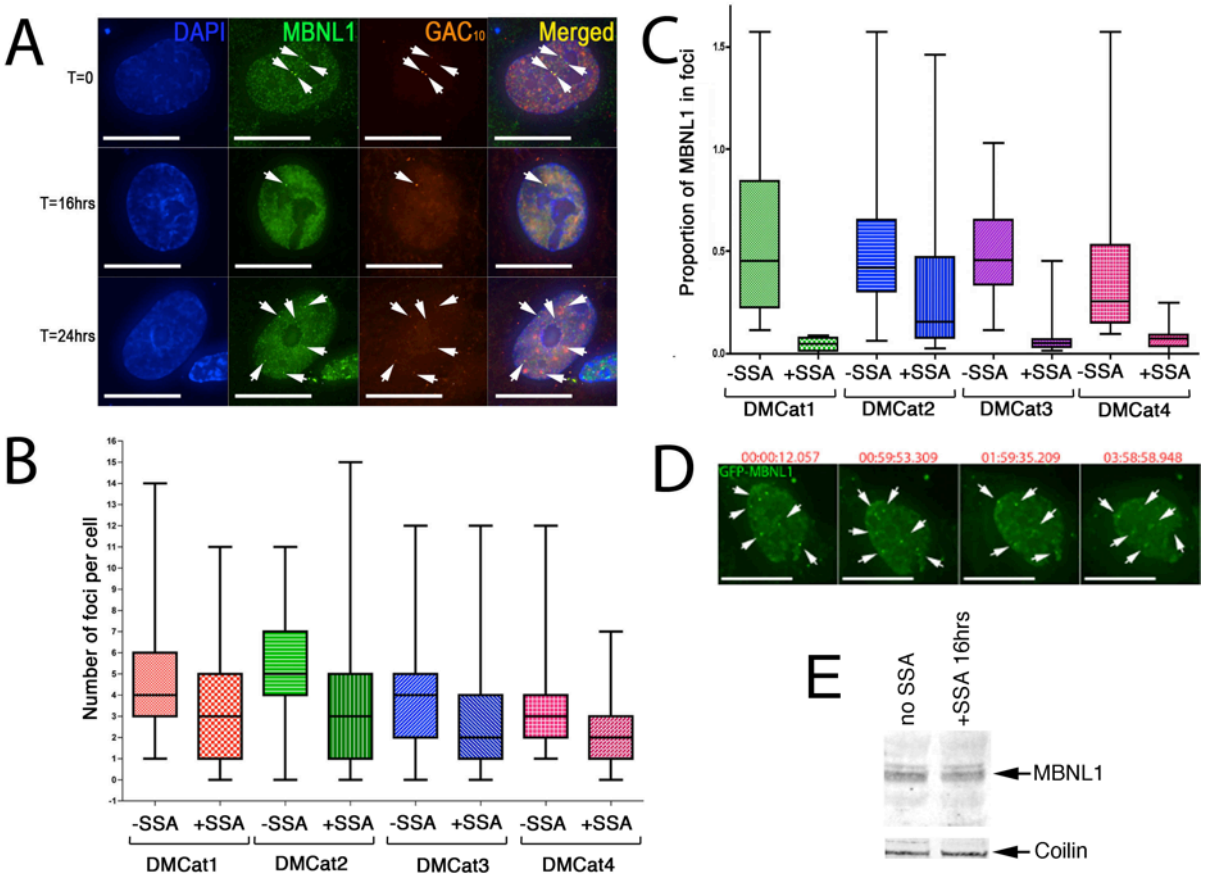
A
DAPI
MBNL1
GAC10
Merged
T=0
T=16hrs
T=24hrs
B
Number of foci per cell
-SSA +SSA -SSA +SSA -SSA +SSA -SSA +SSA
DMCat1 DMCat2 DMCat3 DMCat4
C
Proportion of MBNL1 in foci
-SSA +SSA -SSA +SSA -SSA +SSA -SSA +SSA
DMCat1 DMCat2 DMCat3 DMCat4
D
00:00:12.057
00:59:53.309
01:59:35.209
03:58:58.948
GFP-MBNL1
E
no SSA
+SSA 16hrs
MBNL1
Coilin